Available online at www.sciencedirect.com

SciVerse ScienceDirect

Ceramics International 38 (2012) 2779–2784

CERAMICS INTERNATIONAL

www.elsevier.com/locate/ceramint

Alumina porous nanomaterials obtained by colloidal processing using D-fructose as dispersant and porosity promoter

M. Montero [a], T. Molina [a], M. Szafran [b], R. Moreno [a], M.I. Nieto [a,*]

[a] *Instituto de Cerámica y Vidrio, CSIC, Kelsen 5, E-28049 Madrid, Spain*

[b] *Warsaw University of Technology, Faculty of Chemistry, 00-664 Warsaw, Poland*

Received 31 August 2011; received in revised form 15 November 2011; accepted 16 November 2011

Available online 25 November 2011

Abstract

Recently, great effort has been devoted to obtain porous materials with customized pore size distribution, high surface area and submicrometer sized microstructures or nanostructures. In this work, the viability of colloidal processing routes to obtain porous bulk ceramics using alumina nanopowders and D-fructose as a dispersant and a porosity former has been explored.

The rheological behaviour of nanosuspensions was studied in order to assure their stability and to analyse the influence of different parameters (solids loading, fructose content, pH, sonication time). Mesoporous green bodies were obtained by slip casting with D-fructose in concentrations ranging from 5 to 50 wt%. The drying and burning-out conditions were determined by DTA-TG measurements and the sintering cycles were selected from the dynamic sintering curve. Sintered alumina materials with high porosity (>60%), open microstructures, submicrometer sized porosity (d_p = 140–210 nm) and grain size lower than 500 nm, were obtained for pieces sintered at temperatures of 1300 and 1400 °C. The influence of different processing parameters on the porosity and the microstructure of the sintered materials is discussed.

Published by Elsevier Ltd and Techna Group S.r.l.

Keywords: A. Suspensions; B. Porosity; Alumina; Nanoparticles; D-Fructose

1. Introduction

The properties of porous ceramics, such as high resistance against chemical attack and temperature, low thermal conductivity and high permeability and surface area, make these materials suitable for many applications, including catalysis, biotechnology, electronics, etc. [1–5]. Their properties depend on the morphology, size and distribution of pores and on the level of interconnection among them that defines the permeability and the density as well as the thermo-mechanical properties [6–8].

Various processing routes can be employed to obtain porous ceramic materials, such as partial sintering, sintering of materials with hollow burnable spheres, and sol–gel technology [5], being the principal methods the following: - impregnation of polymeric sponges (polyurethane, polystyrene, cellulose or latex) by a ceramic slurry and subsequent pyrolysis of the polymer [2,9]; - incorporation of organic substances that burn-out during firing (wax, starch) [2,10]; - foaming of ceramic slurries by gas injection (generating gas during a chemical reaction, or by mechanical stirring), and subsequent consolidation by chemical gelcasting [11,12] or using thermal gelling agents [13]; - freeze casting of the ceramic suspensions, using water [14,15] or camphene [16] as a dispersion vehicle.

It is well recognised that nanostructured materials show unusual properties, including enhanced mechanical and electrical properties [17,18], and high surface area and reactivity in the case of porous materials. These properties have a great importance in the design and fabrication of membranes with micro- and mesoporosity for catalytic and filtration applications [19,20]. Consequently, the processing of porous materials with controlled and narrow pore size distribution and high surface area is an interesting topic that is receiving increasing attention. Colloidal processing has demonstrated to be an effective route to overcome the usual problems related to handling and compaction of nanopowders as it allows maintaining particles stabilization during dispersion and shaping steps.

Due to its high surface area and the presence of agglomerates, a great effort has been done to obtain well

* Corresponding author. Tel.: +34 91 7355840; fax: +34 91 7355843.
E-mail address: minieto@icv.csic.es (M.I. Nieto).

0272-8842/$36.00. Published by Elsevier Ltd and Techna Group S.r.l.
doi:10.1016/j.ceramint.2011.11.048

dispersed and stable nanoparticles suspensions [21,22]. In this context, some authors have demonstrated that the addition of some mono- and disaccharides to ceramic suspensions improves fluidity in water [23–26]. It has been reported that the viscosity of alumina nanoparticles suspensions reduced dramatically when adding D-fructose, $C_6H_{12}O_6$ [25]. The structure of D-fructose is shown below:

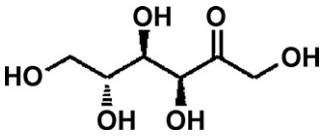

According to Li et al. [24,25], it was found that a significant fraction of water is bound to the surface of powders in aqueous suspensions. When fructose is added, a displacement of this adsorbed water from the alumina surface is produced and, consequently, an increase of free water and water mobility are observed, so that the viscosity is reduced.

More recently, it has been demonstrated that the substitution of $–OCH_3$ group of D-fructose by –OH group increases its deflocculating properties and decreases the viscosity of nano-alumina suspensions [26]. This result is in agreement with the results of Li et al. [24,25] who concluded that the dispersion efficiency of D-fructose is not associated to steric or electrosteric stabilization, but to the decrease of bound water to the particle surface due to the adsorption of the saccharide.

The use of monosaccharides as processing additives has several advantages over other widely used additives [24–28]. They are non-toxic and water-soluble, and they can be easily removed from samples during binder burnout process. Furthermore, the porosity produced during this process can be maintained during firing by designing an adequate sintering cycle. The aim of this work is to obtain porous materials with controlled pore size by colloidal processing of alumina nanopowder using D-fructose as dispersant and porosity former.

2. Experimental

As starting powder, a commercial γ-Al_2O_3 nanopowder (Aeroxide AluC, Degussa-Evonik, Germany) was used, with a surface area of 102 m^2/g, a density of 3.2 g/cm^3, and a calculated d_{BET} of 20 nm, although these nanoparticles are forming agglomerates. D-Fructose (Panreac, Spain), with a density of 1.6 g/cm^3, was selected as a dispersant and porosity promoter. The surface area was measured by multipoint N_2 adsorption (ASAP 2020 Micromeritics, USA) and the density with a He pycnometer (Multipycnometer Quantachrome Corp., USA).

The suspensions were prepared dissolving the adequated amount of fructose in water before alumina powder addition. Concentrations are expressed as wt% with regard to the solid content. Homogenisation was carried out using an ultrasounds probe (Dr. Hielscher 400US, Germany). Zeta potential and particle size measurements were performed by laser Doppler velocimetry (Zetasizer Nano ZS, Malvern S, UK). These determinations were carried out using diluted suspensions and 10^{-2} M KCl as inert electrolyte.

Table 1
composition of studied suspensions.

Sample	Solid loading (vol%)	D-Fructose (wt%) (respect to solids)
5/5	5	5
10/10	10	10
10/15	10	15
10/20	10	20
10/50	10	50
15/50	15	50

The rheological behaviour of suspensions was studied using a rheometer (MARS, Haake, Thermo Electron Co., Germany) with a double-cone/plate sensor configuration. Flow curves were obtained with a three stage measuring program: a linear increase of shear rate from 0 to 1000 s^{-1} in 300 s, a plateau at 1000 s^{-1} for 120 s, and a further decrease to zero shear rate in 300 s. Table 1 shows the composition of the studied suspensions. The influence of the volume fraction of solids, the fructose content and the time of ultrasonic mixing on the flow behaviour was studied.

Green bodies were obtained by slip casting and the drying time in air (72 h) was determined controlling the weight loss of samples. The green density was measured by the Archimedes' method using mercury. In order to evaluate the porosity of green bodies, a nitrogen adsorption isotherm (ASAP 2020, Micromeritics, USA) was determined for the sample 15/50 as a reference for all them. Pore distribution was analysed using the BJH model, considering cylindrical pores (pore diameter is expressed as 4V/A). The porosity was also measured by Mercury Intrusion Porosimetry (Poremaster, Quantachrome Corp., USA). Thermal behaviour was studied by DTA-TG (Exstar 6300, Seiko, Japan) measurements at 10 °C/min, up to 800 °C and air flow 100 mL/min. According to these measurements the conditions for fructose burnout process were established as 500 °C/2 h. Dynamic sintering studies were performed using a differential dilatometer (DI 24, Adamel-Lhomargy, France) in order to select the optimum sintering schedule.

Isothermal sintering was performed at 1300 and 1400 °C for 2 h, with heating and cooling rates of 10 °C/min. The cooling rate is higher than that usually applied for alumina compacts (5 °C/min), but in the case of porous materials, no problems associated to cracking should be expected. The density and the open porosity of sintered pieces were evaluated by Archimedes' method in water. Their pore distribution was measured by Mercury Intrusion Porosimetry (MIP) and the microstructure was studied by field emission scanning electron microscopy, FE-SEM (S-4700, Hitachi, Japan) on fracture surfaces of green and sintered bodies.

3. Results and discussion

The particle size distribution curves of alumina nanosuspensions prepared with different fructose contents were determined before and after sonication. Fig. 1 shows the curves obtained for suspensions containing 5 and 20 wt% of fructose as a function of the applied sonication time. Without US, a bimodal curve

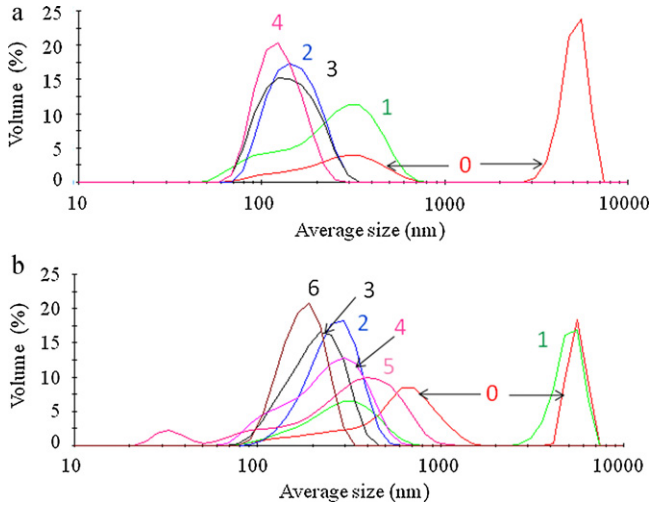

Fig. 1. Particle size distribution curves of alumina nanosuspensions prepared with different fructose contents (a) 5 wt% and (b) 20 wt%, and different sonication times (0, 1, 2, 3, 4, 5 and 6 min).

with big agglomerates having a mean diameter of 2–3 μm is observed in all cases. This peak disappears when ultrasounds are applied and the increase of US time produces a decrease of the mean diameter up to a minimum value obtained after 4 min in all cases, except for the largest fructose content (20%) which requires longer sonication time (6 min) to reach the minimum size, i.e. the maximum dispersion degree. This sonication time of 6 min led to a monomodal size distribution with minimum d_{v50} values ranging from 120 to 180 nm. In the case of lower fructose contents the mode of the curve occurred for particle diameters lower than 100 nm. Nevertheless, these measured values were larger than those calculated from the specific surface area, d_{BET}, which was ~20 nm, indicating that particles are agglomerated for all fructose contents, with an agglomeration factor ranging from 6 to 9 [29].

The zeta potential versus pH curves of alumina without and with 5 wt% of fructose are presented in Fig. 2. The IEP value of the suspension with fructose is near 7.5, lower than that determined for alumina suspension without additives, i.e. 8.5. This suggests that the monosaccharide adsorbs onto the alumina surface, which is in agreement with previous observations of other authors [25]. The zeta potential values

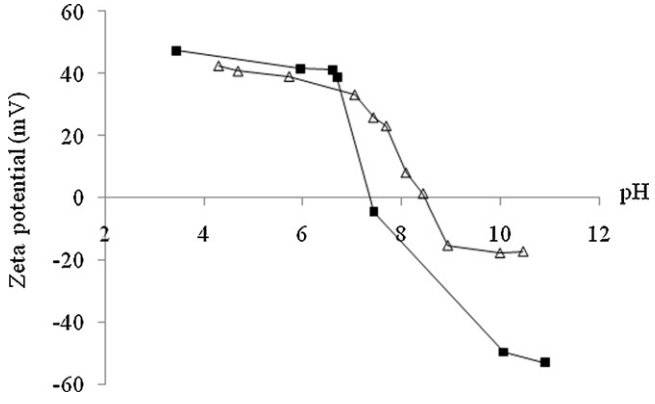

Fig. 2. Zeta potential versus pH curves of alumina without (△) and with 5 wt% of fructose (■).

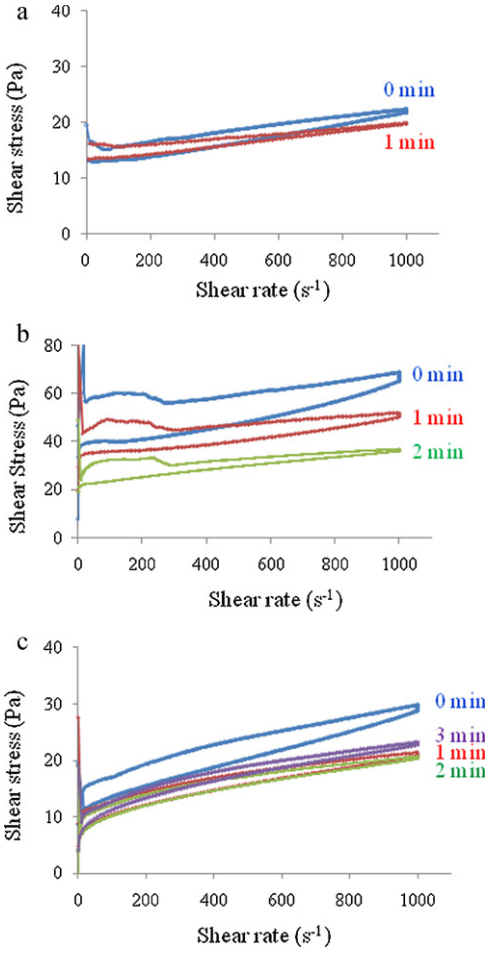

Fig. 3. Flow curves of the suspensions 5/5 (a), 10/20 (b) and 10/50 (c), without and with sonication for 1, 2 or 3 min.

at pH 10–11 are high enough to assure a high stability of the suspensions.

Fig. 3 compares the flow curves obtained for the suspensions prepared to different solids loadings (5 and 10 vol.%) and fructose contents (5, 20, and 50 wt%) homogenised without and with ultrasonication for 1 or 2 min. All suspensions present an important thixotropic cycle, due to the presence of agglomerates. When ultrasounds are applied, both the viscosity and the thixotropy decrease, which can be explained by the breakage of those agglomerates. In all cases, the optimized sonication time was found to be 2 min, and for larger times the viscosity became higher. The increase of the fructose content for constant solids loading (Fig. 3b and c) also produces a decrease on viscosity and thixotropy, thus demonstrating that the addition of fructose to concentrations even higher than the adsorption limit determined by Li and Akinc [25] helps to the stability of these suspensions. The suspensions obtained with fructose are stable and homogeneous and the additive serves two purposes, deflocculant agent on one side, and pore promoter on the other side.

The DTA-TG of pure fructose and 10/50 cast sample are presented in Fig. 4 for comparison purposes. It can be observed that fructose shows some exothermic peaks corresponding to different contributions to weight loss, which associated to different combustion processes, the last one occurring at a

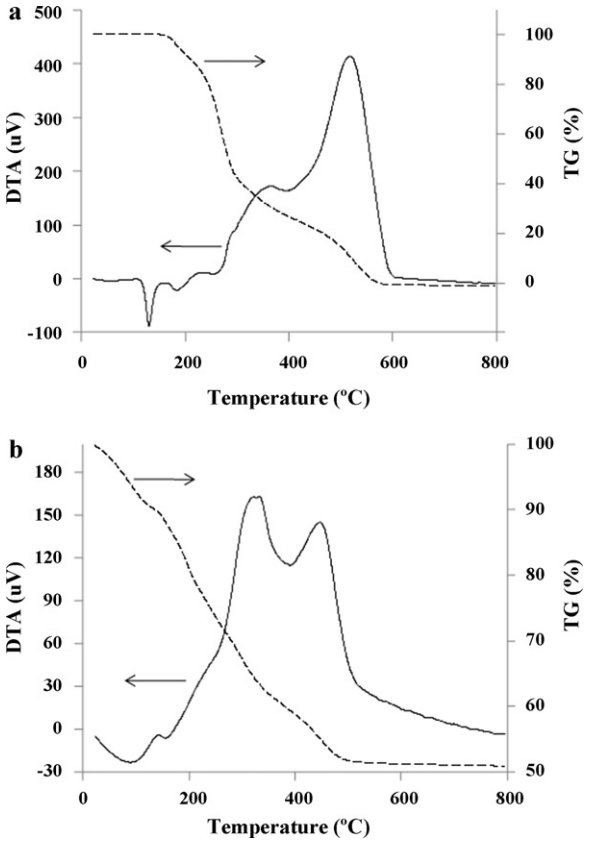

Fig. 4. DTA-TG of pure fructose (a) and 10/50 cast sample (b).

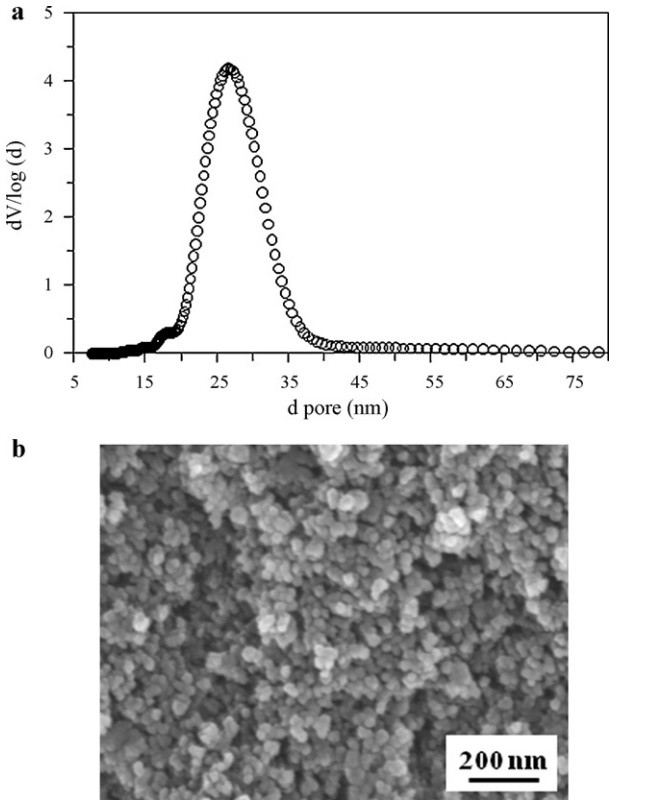

Fig. 5. Pore diameter distribution curve determined by MIP (a) and FE-SEM micrograph (b) for the 10/50 green sample.

temperature of about 530 °C. In the DTA curve of the cast sample, Fig. 4b, similar exothermic peaks are found, although they have different intensity ratios. This fact could be related to the different behaviour of the adsorbed fructose. In this case, the elimination of fructose is completed at 500 °C, as it can be deduced from the TG curve. Consequently, the samples were treated at this temperature to promote fructose burnout.

The weight loss determined after calcinations at 500 °C/2 h and the green densities of thermally treated bodies are presented in Table 2. Weight loss values are always smaller than the fructose content of suspensions. Therefore, some fructose would be eliminated with water during drying and other fraction of fructose remains in the sample, one part adsorbed on the alumina surface and the rest located between the particles; this fraction acts as the porosity promoter agent. Green densities correspond to 25–39% of theoretical density, indicating that the samples have very open microstructures. The pore diameter distribution curve determined by MIP for the 10/50 green sample is shown in Fig. 5, and the data related to porosity determined by both MIP and by N_2 adsorption are reported in Table 3. It is worthy to remark the good agreement between the data obtained with both techniques. The green body is mesoporous, with a mean pore diameter of 23–27 nm, similar to the grain size of the alumina powder, according to an open microstructure, as demonstrated by FE-SEM observations, Fig. 5b.

Table 2
Weight loss and density values of green bodies.

Sample	5/5	10/10	10/20	10/50	15/50
Wt. loss (%)	3	6	12	22	26
ρ (g/cm^3)	0.9	1.0	1.1	1.3	1.4

Table 3
Porosity values of 10/50 sample measured by MIP and N_2 adsorption.

Measurement method	V_p (cm^3/g)	A_p (m^2/g)	d_p (nm)
N_2 adsorption	0.60	105	23 (4V/A)
Hg intrusion porosimetry	0.73	106	27

Dynamic sintering studies were performed with pre-treated bodies (i.e. the fructose was burn-out). Fig. 6 shows the

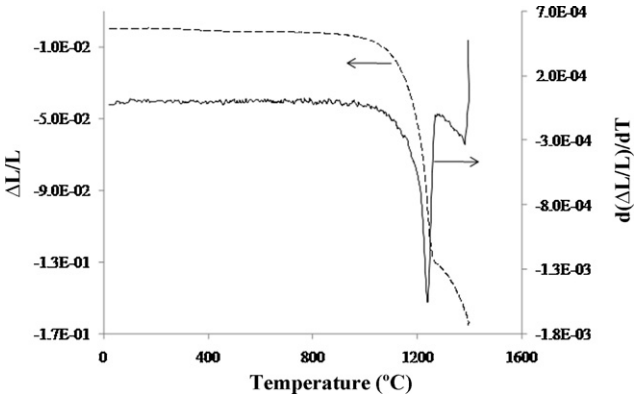

Fig. 6. Dynamic sintering curve performed for the 10/10 sample.

Table 4
Density and porosity values determined by MIP (%, pore volume, area and diameter) of bodies sintered at 1300 and 1400 °C.

Sample	T_{sint} (°C)	% ρ_{th} (±1%)	% porosity (±4%)	V_p (cm^3/g)	A_p (m^2/g)	d_p (nm)
5/5		32	71	0.56	14.6	160
10/10		34	69	0.50	13.2	139
10/20	1300	35	67	0.48	11.8	156
	1400	40	64	0.40	6.6	213
10/50	1300	35	65	0.46	10.0	174
	1400	40	64	0.40	7.9	184
15/50	1300	36	65	0.46	11.5	150
	1400	41	61	0.37	7.2	201

sintering curve obtained for the 10/10 sample. The densification starts at 1000 °C and the peak at 1210 °C, observed in the derivative curve, could be assigned to the transformation of γ to α alumina, with a densification corresponding to the volume change, evaluated as 17% [21]. The densification due to the sintering process is observed at temperatures of 1250 °C and higher. Therefore, the selected temperatures are 1300 and 1400 °C, in order to avoid the grain growth, although from the dilatometry studies it can be seen that full densification is not reached at the studied temperature range.

Densities and porosities of bodies sintered at 1300 °C are presented in Table 4. In the light of the N_2 adsorption isotherm of the 10/50 sample, no mesoporosity is obtained and hence only macropores should be found in the sintered bodies. In Fig. 7, the corresponding pore diameter distribution curves are shown. High porosity (>65%) and narrow and symmetric pore diameter distributions are observed in all cases. When the fructose content is increased, bodies with lower porosity, lower pore volume and lower pore area are found, while the pore size increases. These results are in agreement to the microstructures of the samples observed by FE-SEM on fracture surfaces, Fig. 8. The 10/20 material shows a smoother fracture surface and a more open microstructure than the 10/50 specimen. Furthermore, in the pieces obtained from 50 wt% of fructose, big defects were found, associated to the presence of bubbles in the suspension. Therefore, an optimization of the composition is required in order to design materials with tailored characteristics.

The same behaviour is observed for the bodies sintered at 1400 °C. Their density and porosity values are also presented in

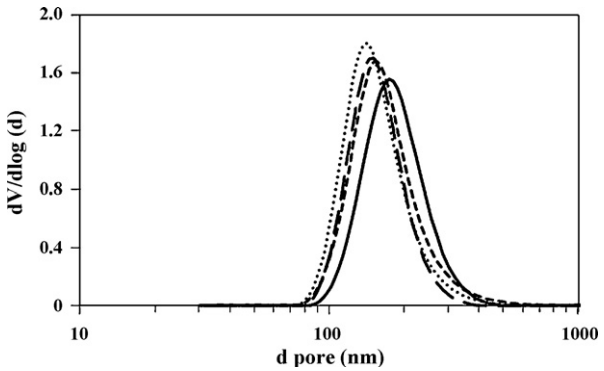

Fig. 7. Pore diameter distribution curves (MIP) for samples sintered at 1300 °C: (• • • •) 10/10, (——) 10/20, (—) 10/50 and (– –) 15/50.

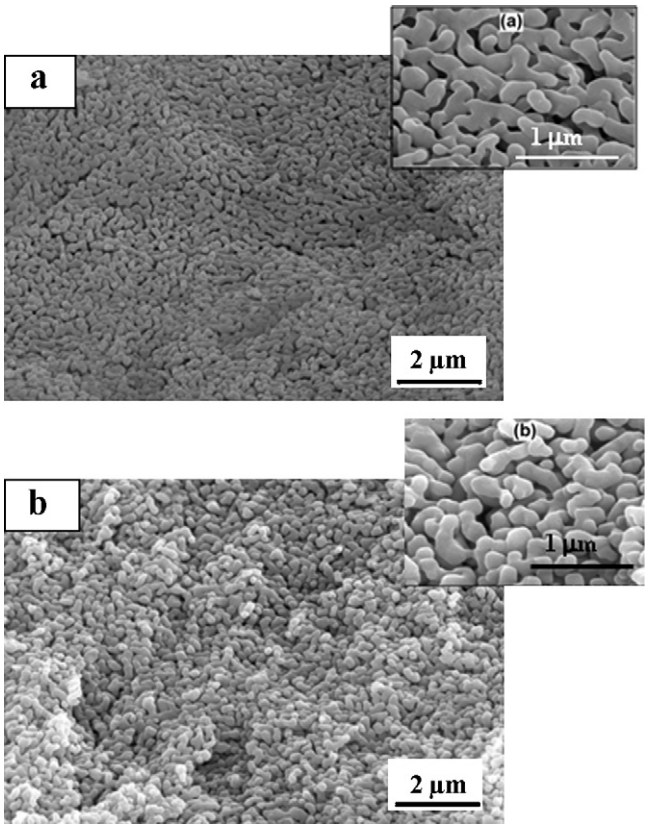

Fig. 8. FE-SEM micrographs on fracture surfaces for samples sintered at 1300 °C: (a) 10/20 and (b) 10/50. Details in the insets.

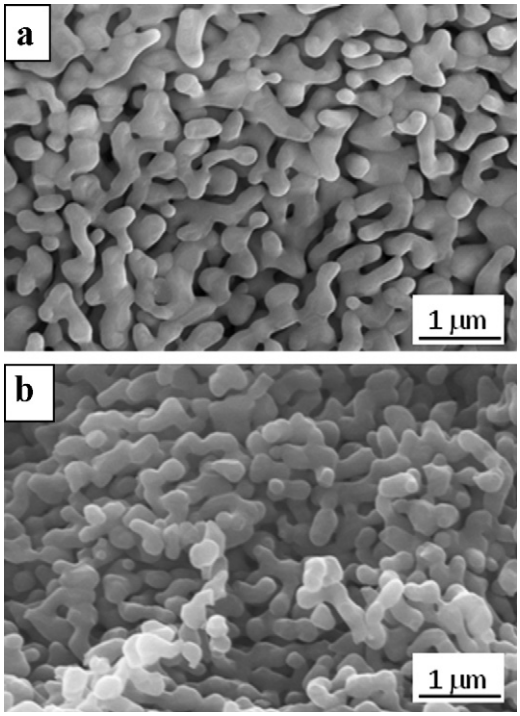

Fig. 9. FE-SEM micrographs on fracture surfaces for samples sintered at 1400 °C: (a) 10/20 and (b) 10/50.

Table 4, and FE-SEM images of fracture surfaces are shown in Fig. 9. As it could be expected, materials sintered at 1400 °C had lower porosity and higher pore diameter, associated to lower pore area than materials sintered at 1300 °C, as well as a significant grain growth. Then, the sintering temperature should be carefully controlled to obtain materials avoiding grain growth and a large concentration of submicrometer size pores.

4. Conclusions

Green mesoporous materials (d_p = 23–27 nm) with a narrow size distribution and a high pore surface area (105 m^2/g) were obtained by colloidal processing of alumina nanopowder with addition of fructose as a deflocculant and pore former.

Sintered materials with high porosity (>60%), open microstructures, grain size lower than 500 nm, with a submicrometer and narrow pore size distribution (d_p = 0.14–0.21 μm) were produced by controlling the sintering temperature. The increase of this temperature promotes an increase of the pore diameter and the grain size significantly increases whereas the area and the volume of pores decrease.

The increase of fructose content reduces the viscosity of nanometric alumina suspensions, but bodies with lower pore volume and pore area as well as higher pore size are obtained. For very high fructose content, the large porosity is associated to an increased number of defects, which could be due to the presence of some bubbles in the suspension.

Acknowledgement

This work has been supported by Spanish Ministry of Science and Innovation (contract MAT2009-14369-C02-01).

References

[1] M. Scheffler, P. Colombo, Cellular Ceramics: Structure, Manufacturing, Properties and Applications, Wiley-VCH, Weinheim, 2005, p. 645.
[2] A.R. Studart, U.T. Gonzenbach, E. Tervoot, L.J. Gauckler, Processing routes to macroporous ceramics: a review, J. Am. Ceram. Soc. 89 (2006) 1771–1789.
[3] P. Sepulveda, J.G.P. Binner, Gelcasting foams for porous ceramics, Am. Ceram. Soc. Bull. 76 (1997) 61–65.
[4] W. Frie, J. Warner, in: F. Schuth, K.S.W. Sing, J. Weitkamp (Eds.), Handbook of Porous Solids Biomedical Applications, vol. 5, Wiley-VCH, Weinheim, 2002, pp. 2923–2970.
[5] C. Galassi, Processing of porous ceramics. Piezoelectric materials, J. Eur. Ceram. Soc. 26 (2006) 2951–2958.
[6] P. Colombo, Engineering porosity in polymer-derived ceramics, J. Eur. Ceram. Soc. 28 (2008) 1389–1395.
[7] F. Tang, H. Fudouzi, T. Uchikoshi, Y. Sakka, Preparation of porous materials with controlled pore size and porosity, J. Eur. Ceram. Soc. 24 (2004) 341–344.
[8] A.E.M. Paiva, P. Sepulveda, V.C. Pandolfelli, Processing and thermomechanical evaluation of fibre-reinforced alumina filters, J. Mater. Sci. 34 (1999) 2641–2649.
[9] J. Luyten, S. Mullens, J. Cooymans, A.M. De Wilde, I. Thijs, New processing techniques of ceramic foams, Adv. Eng. Mater. 5 (2003) 715–718.
[10] O. Lyckfeldt, J.M.F. Ferreira, Processing of porous ceramics by starch consolidation, J. Eur. Ceram. Soc. 18 (1998) 131–140.
[11] P. Sepulveda, J.G.P. Binner, Processing of cellular ceramics by foaming and in situ polymerisation of organic monomers, J. Eur. Ceram. Soc. 19 (1999) 2059–2066.
[12] J.K. Park, J.S. Lee, S.I. Lee, Preparation of porous cordierite using gelcasting method and its feasibility as a filter, J. Porous Mater. 9 (2002) 203–210.
[13] I. Santacruz, M.I. Nieto, R. Moreno, M. Faraldos, E. Sastre, A novel method to prepare zeolites with hierarchical porosity, Adv. Eng. Mater. 7 (2005) 858–861.
[14] S.W. Sofie, F. Dogan, Freeze casting aqueous alumina slurries with glycerol, J. Am. Ceram. Soc. 84 (2001) 1459–1464.
[15] C. Tallón, R. Moreno, M.I. Nieto, Shaping of porous bodies by freeze casting, Adv. Appl. Ceram. 108 (2009) 307–313.
[16] K. Araki, J.W. Halloran, Porous ceramic bodies with interconnected pore channels by a novel freeze casting technique, J. Am. Ceram. Soc. 85 (2005) 1108–1114.
[17] A. Sawaguchi, K. Toda, K. Niihara, Mechanical and electrical-properties of Al_2O_3/SiC nano-composites, J. Ceram. Soc. Jpn. 99 (1991) 523–526.
[18] M. Sternitzke, Structural ceramic nanocomposites, J. Eur. Ceram. Soc. 17 (1997) 1061–1082.
[19] J. Coronas, J. Santamaria, Catalytic reactors based on porous ceramic membranes, Catal. Today 51 (1999) 377–389.
[20] S. Gopalakrishnan, M. Nomura, T. Sugawara, S.I. Nakao, Preparation of a multi-membrane module for high-temperature hydrogen separation, Desalination 193 (2006) 230–235.
[21] P. Bowen, C. Carry, From powders to sintered pieces: forming, transformations and sintering of nanostructured ceramic oxides, Powder Technol. 128 (2002) 248–255.
[22] K. Lu, C. Kessler, Colloidal dispersion and rheology study of nanoparticles, J. Mater. Sci. 41 (2006) 5613–5618.
[23] C.H. Schilling, M. Sikora, P. Tomasik, C. Li, V. Garcia, Rheology of alumina-nanoparticle suspensions: effect of lower saccharides and sugar alcohols, J. Eur. Ceram. Soc. 22 (2002) 917–921.
[24] C. Li, M. Akinc, J. Wiench, M. Pruski, C.H. Schilling, Relationship between water mobility and viscosity of nanometric alumina suspensions, J. Am. Ceram. Soc. 88 (2005) 2762–2768.
[25] C. Li, M. Akinc, Role of bound water on the viscosity of nanometric alumina suspensions, J. Am. Ceram. Soc. 88 (2005) 1448–1454.
[26] P. Falkowski, P. Bednarek, A. Danelska, T. Mizerski, M. Szafran, Application of monosaccharides derivatives in colloidal processing of aluminum oxide, J. Eur. Ceram. Soc. 30 (2010) 2805–2811.
[27] P. Bednarek, Y. Sakka, M. Szafran, T. Mizerski, Gelcasting of alumina with a new monomer synthesized from glucose, J. Eur. Ceram. Soc. 30 (2010) 1795–1801.
[28] M. Szafran, P. Bednarek, T. Mizerski, Monosaccharides derivatives in gelcasting of ceramic powders, in: Proceedings of the E-MRS Fall Meeting, Symposium, 2008, pp. 138–145.
[29] M. Staiger, P. Bowen, J. Ketterer, J. Bohonek, Particle size distribution measurement and assessment of agglomeration of commercial nanosized ceramic particles, J. Disper. Sci. Technol. 23 (2002) 619–630.